Karabük Üniversitesi
DÇE Doğa Bilimleri Dergisi
(NSJ-ISI)
e-ISSN: 2757 8224
Cilt 6, Sayı 1
2025
Araştırma Makalesi

University of Karabuk
ISI Natural Sciences Journal
(NSJ-ISI)
e-ISSN: 2757 8224
Volume 6, Issue 1
2025
Research Article

Performances of HTC@PbS Supercapacitor Electrode Structures

Fatimah Talal Munshid Munshid [1], Fatma Meydaneri Tezel [2]

[1] *Karabük Üniversitesi, Institute of Graduate Studies, Karabük, TÜRKİYE*
[2] *Karabük Üniversitesi, Faculty of Engineering, Karabük, TÜRKİYE*

***Başvuru/Received**: 27 May 2025* ***Kabul / Accepted**: 11 June 2025* ***Çevrimiçi Basım / Published Online:** 01 July 2025*
***Son Versiyon/Final Version**: 30 June 2025*

Öz

Çevre ve ekonomi üzerindeki olumsuz etkileri en aza indirmek ve enerji tüketimini azaltmak amacıyla, gelişmiş, düşük maliyetli ve sürdürülebilir enerji depolama cihazları geliştirmek büyük önem taşımaktadır. Günümüzde süperkapasitörler ve şarj edilebilir bataryalar, iki ana umut vadeden enerji depolama çözümü olarak öne çıkmaktadır. Yüksek performanslı elektrokimyasal enerji depolama sistemleri üretmenin anahtarı, elektrokimyasal olarak aktif malzemelerdir. Elektrokimyasal performanslarını artırmak amacıyla, geniş spesifik yüzey alanına ve kontrol edilebilir gözenek boyutlarına sahip gözenekli yapılar tasarlamak gerekmektedir. Bu çalışmada, hidrotermal karbon (HTC) katkılı kurşun sülfür (HTC@PbS) ince film süperkapasitör elektrot yapıları, sprey yöntemiyle 100 °C'deki cam taban malzemeleri üzerine, sprey sayısına bağlı olarak üretilmiştir. Yüzey morfolojileri, bileşim analizleri ve kristal yapıları sırasıyla FESEM, EDX ve XRD ile karakterize edilmiştir. 2 puf ve 3 puf HTC@PbS ince film süperkapasitör elektrot yapılarının spesifik kapasitans (Cs) değerleri, Keithley 2400 sourcemeter ve 2100/220 Keithley multimetre kullanılarak, düzlemsel zamana bağlı I-V yöntemi ile -1,4 V ile +0,2 V potansiyel aralığında, 5 mV/s, 10 mV/s, 25 mV/s, 50 mV/s ve 100 mV/s tarama hızlarında ölçülmüştür. 2 puf ve 3 puf HTC@PbS ince film süperkapasitör elektrot yapılarında kaplanan aktif kütle miktarları sırasıyla 0,0566 g ve 0,0185 g olarak belirlenmiştir. 2 puf ve 3 puf sprey için 5 mV/s tarama hızında elde edilen spesifik kapasitans değerlerinin 873 F/g ve 919 F/g olarak en yüksek değerlere sahip olduğu görülmektedir.

Anahtar Kelimeler

Kurşun Sülfür, Hidrotermal Karbon, Enerji Depolama, Süperkapasitör Elektrot, Spesifik Kapasitans

Abstract

To mitigate adverse environmental and economic impacts and to reduce energy consumption, the development of innovative, affordable, and sustainable energy storage systems is crucial. Currently, rechargeable batteries and supercapacitors are recognized as the two leading energy storage solutions. The production of high-performance electrochemical energy storage systems relies heavily on electrochemically active materials. To enhance their electrochemical capabilities, it is essential to create porous structures featuring a high specific surface area and adjustable pore dimensions. In this study, hydrothermal carbon (HTC) doped lead sulfide (HTC@PbS) thin film supercapacitor electrode structures were fabricated on glass substrates at 100 °C using the spray method, with their properties varying depending on the number of sprays. Surface morphologies, compositional analyses, and crystal structures were characterized by FESEM, EDX mapping, and XRD, respectively. The specific capacitance (Cs) values for the 2- and 3-spray HTC@PbS thin film supercapacitor electrode structures were measured using the in-plane time-dependent I-V method, employing a Keithley 2400 sourcemeter and a Keithley 2100/220 multimeter. Measurements were conducted in the potential range of -1.4 V to +0.2 V at scan rates of 5 mV/s, 10 mV/s, 25 mV/s, 50 mV/s, and 100 mV/s. For the 2- and 3-spray HTC@PbS thin film supercapacitor electrode structures, the amount of active mass coated was determined to be 0.0566 g and 0.0185 g, respectively. The specific capacitance values for the 2- and 3-spray samples, measured at a 5 mV/s scan rate, showed the highest values of 873 F/g and 919 F/g.

Key Words

Lead sulfide, Hydrothermal Carbon, Energy Storage, Supercapacitor Electrode, Specific Capacitance

***Corresponding Author:** fatmameydaneri@karabuk.edu.tr*

1. Introduction

Energy is acknowledged as a vital element for the advancement and economic health of contemporary society around the globe. Nonetheless, the rising consumption of energy in recent years has resulted in issues like the exhaustion of fossil fuel resources and environmental degradation [1,2]. It is essential to transition from traditional energy sources to alternative renewable energy options. Over the past two to three decades, substantial global efforts have been dedicated to the research and development of diverse renewable energy sources to meet energy demands while minimizing environmental impact. Renewable energy types, including biomass, solar, wind, and hydroelectric power, have been recognized as viable prospects. Among the different pretreatment techniques, hydrothermal carbonization (HTC) has proven to be an effective approach for enhancing physicochemical characteristics [3,4].

With the discovery of nanoporous carbons as a functional class of materials, their potential applications such as supercapacitors, H_2 storage, CO_2 capture, photocatalysis, etc. continue to increase greatly. Carbon can form sp, sp^2, and sp^3 bonds, as it uniquely lacks any internal p-electrons. Consequently, it can display distinct characteristics with various allotropic forms that range from nanoscopic to macroscopic sizes, along with numerous nanostructured configurations, which influence their physicochemical properties such as electrical conductivity, low weight, porosity, and chemical stability across different scales. The remarkable traits of carbon, particularly those that are activated, are greatly affected by the diverse range of surface functionalities that include heteroatoms. A straightforward method to adjust and regulate the physicochemical properties of carbon substances must be developed to leverage them for cutting-edge uses [5]. There are two primary and often interrelated approaches to easily manage the qualities of porous carbon: creating the pore structure and adding specific functional groups to the carbon surface and matrix [6,7]. While significant advancements have been achieved in producing nanoporous carbons with innovative shapes [8], heteroatom-doped carbons (HDCs) featuring adjustable structural and chemical attributes have gained more attention due to their multifaceted capabilities, especially as sophisticated functional materials [9,10]. Specifically, HDCs with well-defined porosity and extensive surface area demonstrate enhanced effectiveness for energy storage and conversion applications in fuel cells, supercapacitors, and batteries, as well as for CO_2 capture and hydrogen storage [11].

Advancements in the modern electronics industry are closely tied to progress in the technology of semiconductor materials. Components of electronic circuits made from semiconductors are essential in various aspects of daily life. These semiconductor components are utilized in fields such as communication, healthcare, information technology, automotive, transportation, military, and several others. Systems built with semiconductors offer benefits like being lightweight, compact, possessing low error rates, cost-effective, and highly efficient. The construction of each discrete solid-state electronic device or integrated circuit starts with the production of high quality semiconductor materials. Lead sulfide (PbS) is an important component among semiconductor materials and is utilized in a wide range of applications due to its remarkable physical and chemical characteristics. These applications include light emitting diodes (LEDs), infrared sensors, lasers, solar energy systems, optical fibers, and window coverings, all thanks to its ability to act as a Pb^{+2} ion-selective sensor [12-14]. PbS is a distinctive semiconductor with a direct energy band gap of 0.41 eV at ambient temperature, classified under group IV-VI of the periodic table [15]. Furthermore, PbS exhibits a cubic crystal structure, possesses a dielectric constant of 17.3, and has a significant exciton and effective Bohr radius of 18 nm [16,17]. Its strong ability to absorb in the infrared (IR) range and into the visible spectrum makes it ideal for applications in IR detection [18]. Recently, nanoparticles for PbS material have been further developed physically and chemically. Due to the quantum confinement of the carriers, it has been discovered that the ternary non-linear optical properties are strong, which suggests that it can be used as an optical switch in optical circuits [19]. Moreover, various metals and heteroatoms are doped into PbS nanostructures to improve their physical, chemical, optoelectronic, etc. properties for different applications. In this study, our aim is to fabricate spray number dependent HTC@PbS thin film supercapacitor electrodes by doping hydrothermal carbon (HTC) and to discuss the effective parameters by revealing the relationship between specific capacitance values and structural characterisation.

2. Experimental Section

The experiment consists of 3 stages. The first stage is the production of hydrothermal carbons, the second stage is the preparation of HTC@PbS solution and the last stage is the growth of HTC@PbS thin film supercapacitor electrodes depending on the spray number.

Firstly, 8 g of glucose is added to 80 ml of pure water in a 100 ml beaker and mixed at 600 rpm for 5 mins. with a magnetic stirrer. Then, it is continued to be stirred in ultrasonic mixer for 15 mins. at room temperature and the solution is placed in autoclave and kept in oven at 180 °C for 18 hours. After cooling, it is removed from the oven, filtered, washed with distilled water and finally kept in an oven at 50 °C until drying to obtain HTCs.

In the second step, 0.02 Molar $PbNO_3$ in 20 ml distilled water is stirred in a magnetic stirrer for 30 mins. at room temperature. In another beaker, 0.648 g NaOH in 10 ml distilled water is stirred at room temperature for 20 mins. and then the solution in both beakers is taken into a 100 ml beaker, and stirred for 10 mins. to obtain a homogeneous solution. In another beaker, 0.002 g of HTC in 20 ml of distilled water was stirred at 100 °C and 500 rpm for 5 hours in a magnetic stirrer and added to 100 ml of solution. In another beaker, 0.05 Molar thiourea [$(NH_2)_2CS$] was stirred in 10 ml of distilled water at room temperature for 10 mins. on a magnetic stirrer and added dropwise into 100 ml of the mixture with the help of a micropipette and stirred on a magnetic stirrer for 30 mins. During this time the colour of the solution changed towards dark grey colour.

In the last stage, when the temperatures of the glass substrates placed on the heater by weighing their empty masses reached 100 °C, the distance between the glass substrates and the nozzle at right angles to the surface was adjusted to 10 cm and HTC@PbS thin films were produced for 2 and 3 sprays with air gas and the amount of active material mass coated was measured with a precision balance.

Surface morphologies, compositional analyses and crystal structures were characterised by FESEM, EDX mapping and XRD, respectively. The specific capacitance (Cs) values of HTC@PbS thin film supercapacitor electrode structures produced with 2 and 3 sprays were measured by in-plane time-dependent I-V method using Keithley 2400 sourcemeter and 2100/220 Keithley multimeter in the potential range of -1.4 V to +0.2 V at scan rates of 5 mV/s, 10 mV/s, 25 mV/s, 50 mV/s and 100 mV/s.

3. Results and Discussion

XRD patterns of HTC@PbS thin film supercapacitor electrode structures depending on the number of 2 and 3 sprays are given in Figure 1. Accordingly, the formation of cubic PbS crystals having a=b=c=5.9300 Å with (1 1 1 1), (1 1 1 1), (2 0 0), (2 2 2 0) and (3 1 1) Miller planes at diffraction angles of 23.39°, 26.03°, 30.17°, 43.47° and 50.98°, respectively, was observed (PDF Card No.: 00-002-0699). In addition, the formation of orthorhombic crystalline $PbSO_4$ having crystal structure parameters a=8.4500 Å, b=5.3800 Å, c=6.9300 Å with (2 1 1) and (2 1 2) Miller planes at diffraction angles of 29.76° and 37.44° (PDF Card No.: 00-001-0867), respectively, was observed during the reaction. Miller planes (1-10), (110) and (200) at 2θ=14.8°, 16.8° and 22.6° diffraction angles, respectively, indicate HTC structures [20].

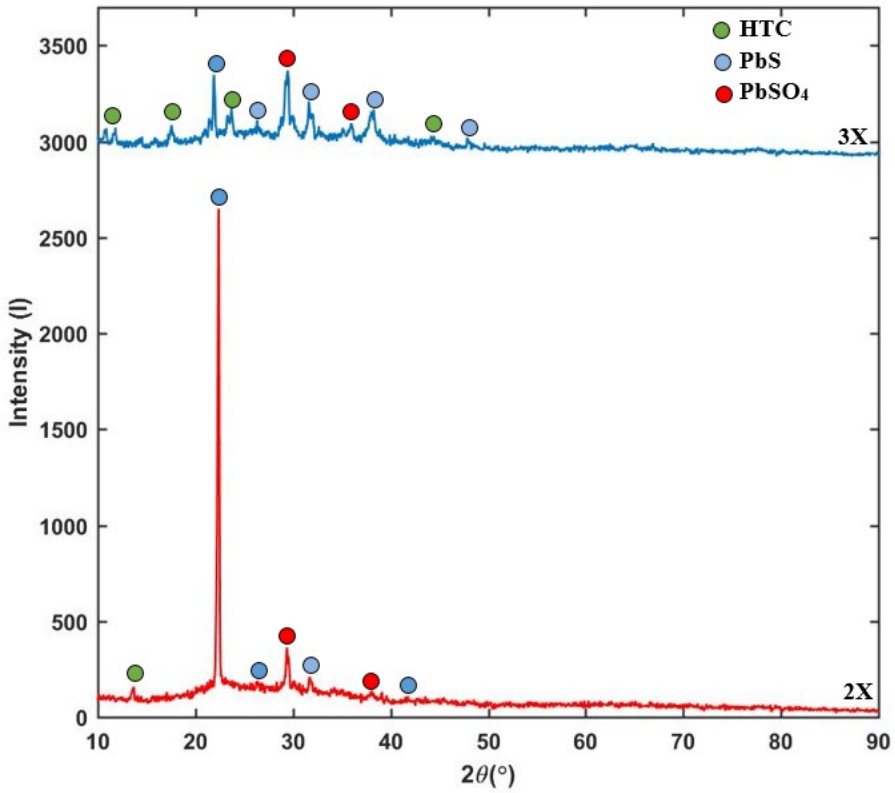

Figure 1. XRD patterns of HTC@PbS thin film supercapacitor electrodes depend on spray numbers.

Surface morphologies and EDX mapping analyses of HTC@PbS thin film supercapacitor electrode structures produced for 2 and 3 sprays are depicted in Figure 2. According to this, the temperature of the glass substrate materials at 100 °C shows that the films have a dense and homogeneous surface morphology. In 2x spray, some parts of the surface appear as hollow, small spheres and layered adhesive network, while in 3x spray, some parts of the film are in the form of small spheres, but in some parts of the film, the formation of grain structures similar to small cauliflower branches is observed. In addition, the presence of regions with excessive glow on the surface in the FESEM image in the 3x supercapacitor electrode structure indicates that oxidation is excessive, which is clearly seen from EDX mapping and XRD diffraction patterns.

The masses of the base material glasses before and after spraying were weighed with a precision balance and the amount of active material used in the calculation of the specific capacitance values was determined. Accordingly, the amount of active substance was measured as 0.0566 g and 0.0185 g for 2x and 3x HTC@PbS spray, respectively. Specific capacitance (Cs) values of 2x and 3x HTC@PbS thin film supercapacitor electrode structures were measured with the help of Keithley 2400 sourcemeter and 2100/220 Keithley multimeter using in-plane time-dependent I-V method with Kickstart programme at scan rates of 5 mV/s, 10 mV/s, 25 mV/s, 50 mV/s and 100 mV/s in the potential range of -1.4V to +0.2V. Since PbS crystals are sensitive to temperature and light, all measurements were performed at room temperature and in the dark.

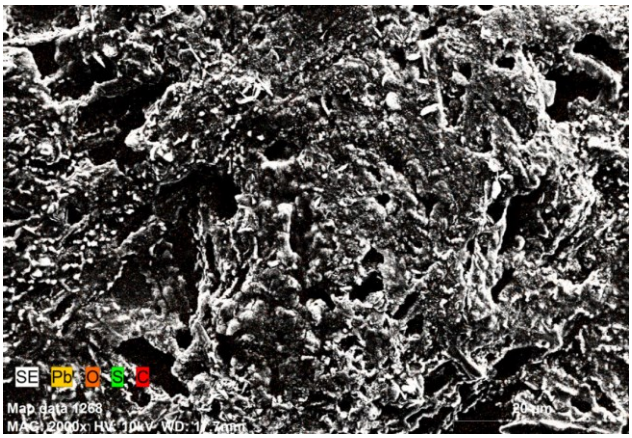
SE Pb O S C
Map data 1268
MAG: 2000x HV: 10kV WD: 17.7mm
20 µm

a)

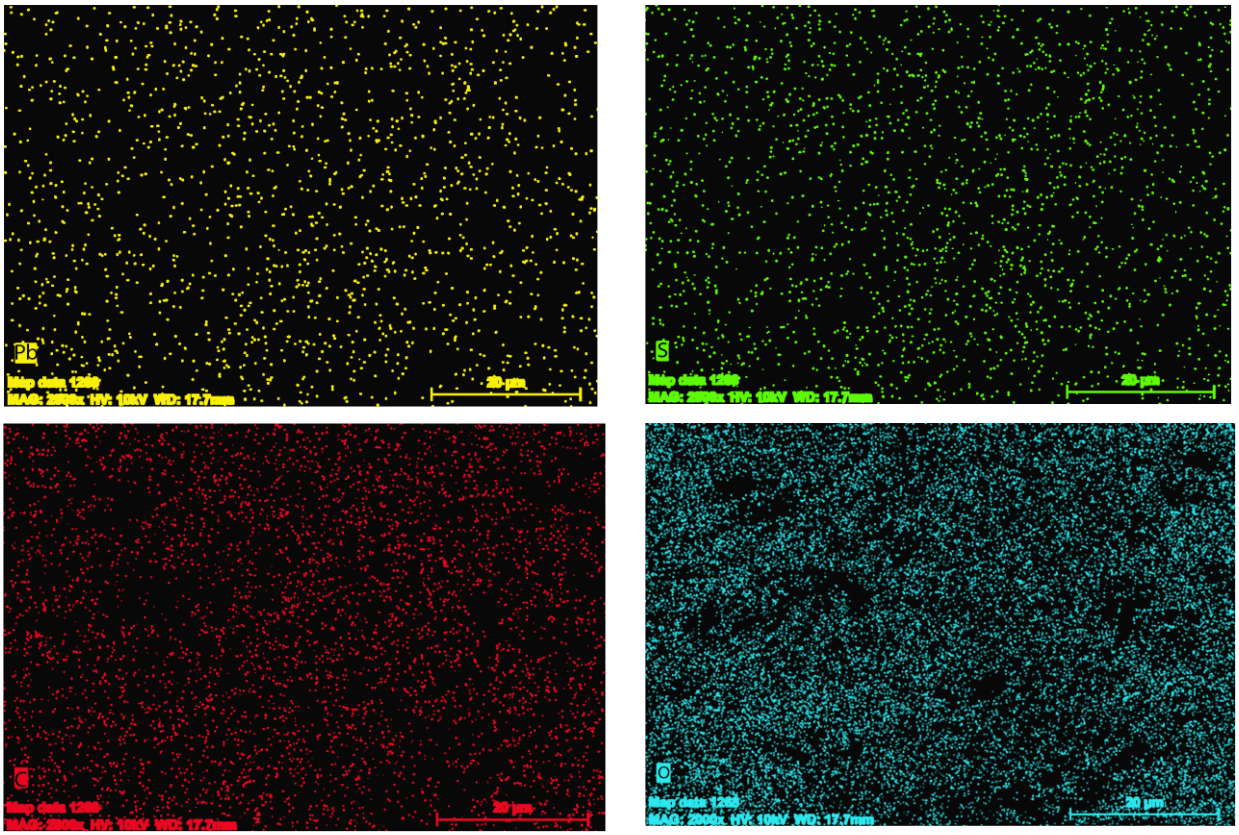
Pb
S
C
O

b)

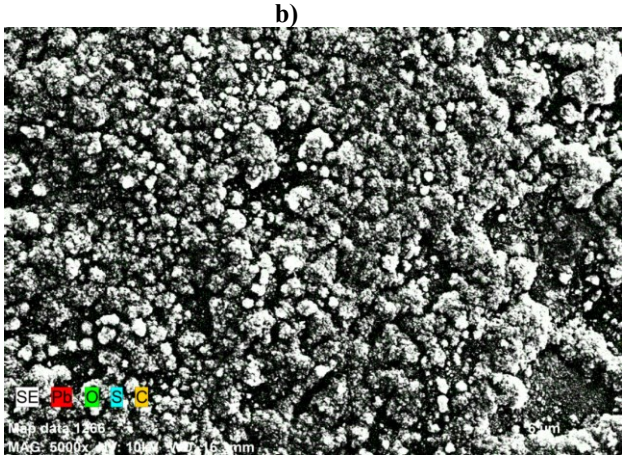
SE Pb O S C
Map data 1268
MAG: 5000x HV: 10kV WD: 16.5mm
5 µm

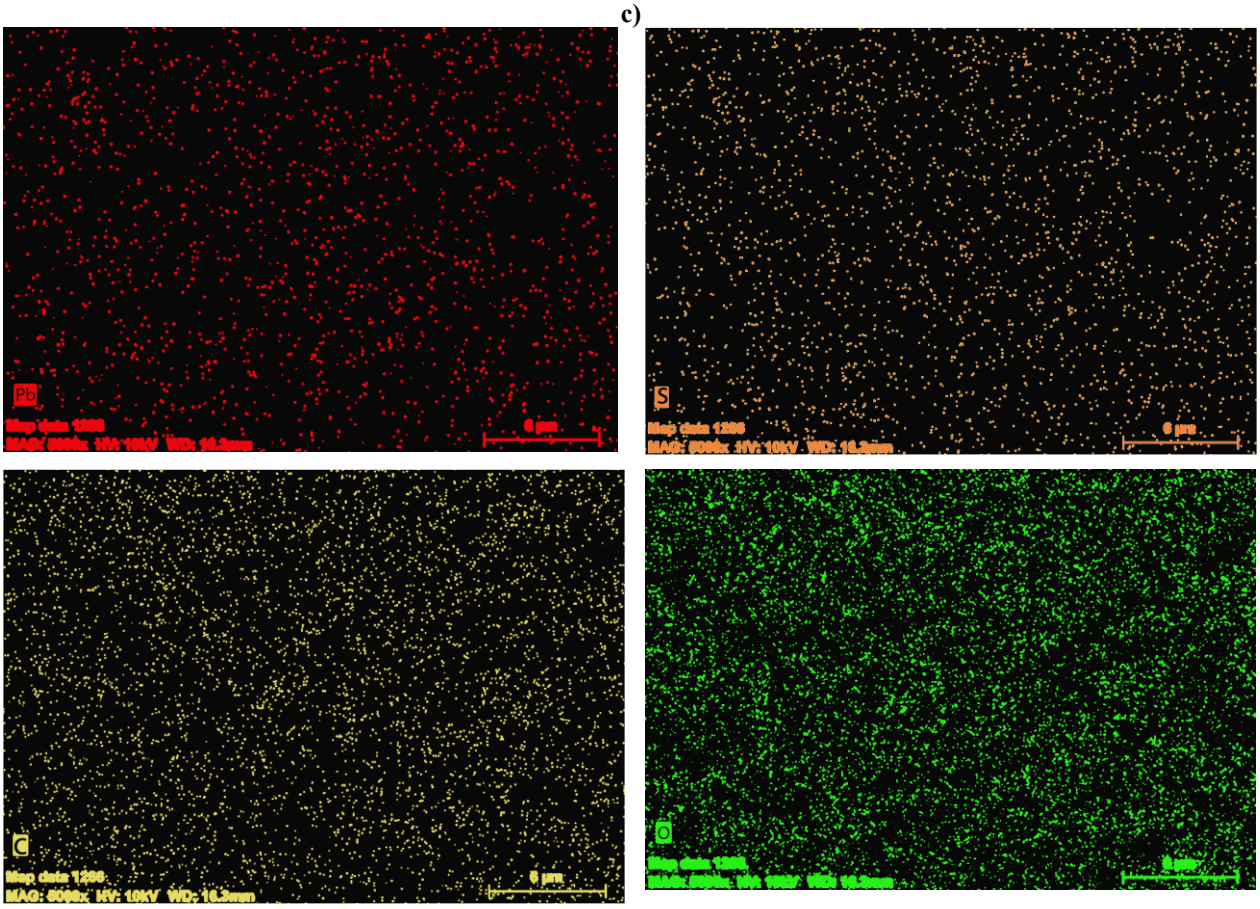

Figure 2. FESEM images and EDX mappings of HTC@PbS thin film supercapacitor electrodes depends on sprey amounts (a)2X FESEM image, b) 2X EDX Mapping, c)3X FESEM image, d) 3X EDX Mapping)

The specific capacitance values were calculated by using the amount of active material coated and I-V values with the help of Equation 1 [21-23].

$$C_S = \frac{I}{m.\frac{dV}{dt}} \quad (1)$$

where Cs is specific capacitance (F/g), I is current (A), m is the amount of active substance coated (g). For 2 and 3 times spraying, cyclic voltammetry curves for 5, 10, 25, 50 and 100 mV/s scan rates are given in Figure 3 and calculated Cs values are given in Table 1. Accordingly, Cs values decrease with increasing scan rates, whereas Cs values are higher since the amount of active mass decreases in the 3x sample. High specific capacitance (Cs) values are obtained at low scan rates due to the excitation of more charge from the surface to the interior of the active material at low potentials scanned per unit time, i.e. due to the interaction of only surface charges at high scan rates. In addition, the increase in the mass of the active material at 2x caused a decrease in the specific capacitance values due to the decrease in the free path that the charges settled in the pores of the HTC will take in the electrical field formed with the applied potential. At the lowest scan rate of 5 mV/s, Cs values of 873 F/g and 919 F/g were obtained for 2x and 3x sprays, respectively. Durga and colleagues [24] observed specific capacitance figures ranging from 248.48 F/g to 41.4 F/g for PbS supercapacitor electrodes created on Ni foam using the chemical bath deposition technique, which are significantly less than the values reported in this research. The reason for this is thought to be due to the method applied, the substrate material, the amount of active material and the pores of the doped HTC. In addition, another situation is that with the formation of $PbSO_4$ crystal structures in the synthesis stage obtained in this study, oxygen acts as a heteroatom in the structure and increases the specific capacitance values. Mohamed et al. [25] found the specific capacitance value of PbS flake nanostructured supercapacitor electrodes hydrothermally deposited on graphene oxide sheets as 1371.57 F/g as a result of three-electrode method. In addition, for PbS@GO//AC (activated carbon) structured asymmetric supercapacitor, they reached a specific capacitance value of 251 F/g for 1 A/g, which is in agreement with the specific capacitance values obtained in this study.

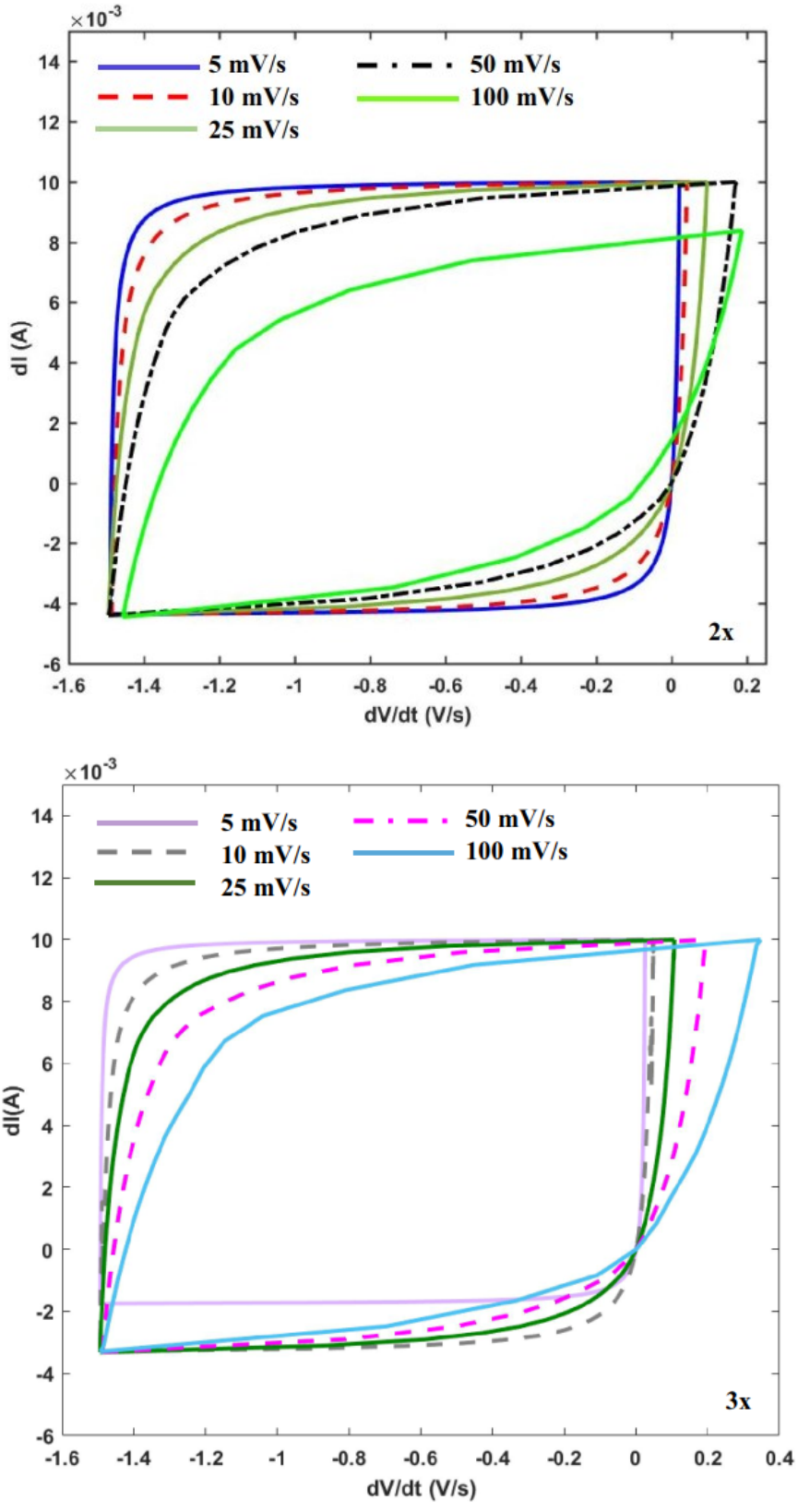

Figure 3. Cyclic voltammetry curves of HTC@PbS thin film supercapacitor electrodes structures depend on scanning rate for 2x and 3x sprays.

Table 1. Specific capacitance values depend on scanning rates for HTC@PbS thin film supercapacitor electrodes.

	Scan Rate (mV/s)	C, Specific Capacitance (F/g)
2 x	5	873
	10	442
	25	193
	50	111
	100	59
	Scan Rate (mV/s)	**C, Specific Capacitance (F/g)**
3 x	5	919
	10	880
	25	707
	50	464
	100	276

4. Conclusion

In this research, HTC-infused PbS thin film supercapacitor electrodes were created on glass substrates at a temperature of 100 °C using a spray technique that is straightforward, affordable, and requires minimal equipment based on two and three spray applications. Their surface structure appears quite compact, resembling tiny spherical particles. The emergence of $PbSO_4$ crystals within the composition and the role of oxygen as a foreign atom played crucial roles in enhancing the specific capacitance values. An increase in the scanning rate led to a decrease in specific capacitance values, as only surface charges were engaged. Due to the high density of carriers in the PbS chalcogenide structure and the enhanced number of pores on the surface resulting from the additional HTC, supercapacitors that are cost-effective, easy to manufacture, environmentally benign, and exhibit high performance with appropriate size and structure can be produced and further improved with additives.

Acknowledgement

This study was supported by Karabük University Scientific Research Projects Coordination with the project code KBÜBAP-25-YL-020. The authors would like to thank the KBÜ-BAP unit for their financial support. We would also like to thank Karabük University Iron and Steel Institute for the equipment used during the experimental studies.

References

[1] Pandey, V. K., Verma, S., & Verma, B. (2022). Polyaniline/activated carbon/copper ferrite (PANI/AC/CuF) based ternary composite as an efficient electrode material for supercapacitor. *Chemical Physics Letters*, *802*, 139780.

[2] Pandey, V. K., Verma, S., Das, T., & Verma, B. (2022). Supercapacitive behavior of polyaniline-waste derived carbon-copper cobaltite based ternary composite. *Bioresource Technology Reports*, *20*, 101255.

[3] Islam, M. A., Asif, M., & Hameed, B. H. (2015). Pyrolysis kinetics of raw and hydrothermally carbonized Karanj (Pongamia pinnata) fruit hulls via thermogravimetric analysis. *Bioresource technology*, *179*, 227-233.

[4] Nawaz, A., & Kumar, P. (2023). Impact of temperature severity on hydrothermal carbonization: fuel properties, kinetic and thermodynamic parameters. *Fuel*, *336*, 127166.

[5] Maiti, U. N., Lee, W. J., Lee, J. M., Oh, Y., Kim, J. Y., Kim, J. E., ... & Kim, S. O. (2014). 25th anniversary article: chemically modified/doped carbon nanotubes & graphene for optimized nanostructures & nanodevices. *Advanced Materials*, *26*(1), 40-67.

[6] Stein, A., Wang, Z., & Fierke, M. A. (2009). Functionalization of porous carbon materials with designed pore architecture. *Advanced Materials*, *21*(3), 265-293.

[7] Li, Z., & Dai, S. (2005). Surface functionalization and pore size manipulation for carbons of ordered structure. *Chemistry of materials*, *17*(7), 1717-1721.

[8] Chuenchom, L., Kraehnert, R., & Smarsly, B. M. (2012). Recent progress in soft-templating of porous carbon materials. *Soft Matter*, *8*(42), 10801-10812.

[9] Shen, W., & Fan, W. (2013). Nitrogen-containing porous carbons: synthesis and application. *Journal of Materials Chemistry A*, *1*(4), 999-1013.

[10] Paraknowitsch, J. P., & Thomas, A. (2017). Functional carbon materials from ionic liquid precursors. *Chemical Synthesis and Applications of Graphene and Carbon Materials*, 21-42.

[11] Kiciński, W., Szala, M., & Bystrzejewski, M. (2014). Sulfur-doped porous carbons: Synthesis and applications. *Carbon*, *68*, 1-32.

[12] Ni, Y., Liu, H., Wang, F., Liang, Y., Hong, J., Ma, X., & Xu, Z. (2004). PbS crystals with clover-like structure: Preparation, characterization, optical properties and influencing factors. *Crystal Research and Technology: Journal of Experimental and Industrial Crystallography*, *39*(3), 200-206.

[13] Peterson, J. J., & Krauss, T. D. (2006). Fluorescence spectroscopy of single lead sulfide quantum dots. *Nano letters*, *6*(3), 510-514.

[14] Chandekar, K. V., Alkallas, F. H., Trabelsi, A. B. G., Shkir, M., Hakami, J., Khan, A., ... & AlFaify, S. (2022). Improved linear and nonlinear optical properties of PbS thin films synthesized by spray pyrolysis technique for optoelectronics: An effect of Gd3+ doping concentrations. *Physica B: Condensed Matter*, *641*, 414099.

[15] Hone, F. G., Dejene, F. B., & Echendu, O. K. (2018). Band gap tailoring of chemically synthesized lead sulfide thin films by in situ Sn doping. *Surface and Interface Analysis*, *50*(6), 648-656.

[16] Zhou, S. M., Feng, Y. S., & Zhang, L. D. (2003). Sonochemical synthesis of large-scale single-crystal PbS nanorods. *Journal of materials research*, *18*(5), 1188-1191.

[17] Machol, J. L., Wise, F. W., Patel, R. C., & Tanner, D. B. (1993). Vibronic quantum beats in PbS microcrystallites. *Physical Review B*, *48*(4), 2819.

[18] Moss, T. S. (2007). Lead salt photoconductors. *Proceedings of the IRE*, *43*(12), 1869-1881.

[19] Kane, R. S., Cohen, R. E., & Silbey, R. (1996). Theoretical study of the electronic structure of PbS nanoclusters. *The Journal of Physical Chemistry*, *100*(19), 7928-7932.

[20] Teh, S. J., Hamid, S. B. A., Lai, C. W., & Lim, Y. S. (2015). $ZnCl_2$/NaCl-catalysed hydrothermal carbonization of glucose and oil palm shell fiber. *Nanoscience and Nanotechnology Letters*, *7*(7), 611-615.

[21] Tezel, N. S., Korkmaz, S., Meydaneri Tezel, F., Kariper, İ. A. (2021). Synthesis and Characterization of $Sn_3Sb_2S_6$Thin Film Supercapacitor Electrodes: The Effect of Deposition Temperature. Academic Research & Reviews In Engineering, Chapter 4, pp.45-65, ISBN: 978-625-7721-50-9, Serüven Publishing, İzmir/Turkey.

[22] Tezel, N. S., Tezel, F. M., & Kariper, I. A. (2021). Effects of pH on the optical, structural and supercapacitive properties of BiTe thin films produced via CBD. *Bulletin of Materials Science*, *44*(2), 150.

[23] Kariper, İ. A., & Tezel, F. M. (2019). UV region supercapacitor: Bi-doped natural MgO rock salt thin film. *Ceramics international*, *45*(7), 9219-9224.

[24] Kanaka Durga, I., Srinivasa Rao, S., Ahn, J. W., Park, T. Y., Jin-Soo, B., Ho, C. I., ... & Kim, H. J. (2018). Dice-like nanostructure of a CuS@ PbS composite for high-performance supercapacitor electrode applications. Energies, 11(7), 1624.

[25] Kashif, M., Khan, S., Wajahat, H., Alharbi, F. F., Al-Sehemi, A. G., Eman, S., & Alqurashi, H. (2024). Physicochemical and electrochemical investigation of lead sulphide-graphene oxide hybrid nanostructure for energy storage applications. *Journal of Electroanalytical Chemistry*, *974*, 118680.